

FuzzCoh: Robust Canonical Coherence-Based Fuzzy Clustering of Multivariate Time Series

Ziling Ma ^{1,*}, Mara Sherlin Talento ^{1,*}, Ying Sun ¹, Hernando Ombao ¹

SUMMARY: Brain cognitive and sensory functions are often associated with electrophysiological activity at specific frequency bands. Clustering multivariate time series (MTS) data like EEGs is important for understanding brain functions but challenging due to complex non-stationary cross-dependencies, gradual transitions between cognitive states, noisy measurements, and ambiguous cluster boundaries. To address these issues, we develop a robust fuzzy clustering framework in the spectral domain. Our method leverages the Kendall’s tau-based canonical coherence (KenCoh) which extracts meaningful frequency-specific monotonic relationships between groups of channels or regions. KenCoh effectively captures dominant coherence structures while remaining robust against outliers and noise, making it suitable for real EEG datasets that typically contain artifacts. Our method first projects each MTS object onto vectors derived from the KenCoh estimates (i.e, canonical directions), which capture relevant information on the connectivity structure of oscillatory signals in predefined frequency bands. These spectral features are utilized to determine clusters of epochs using a fuzzy partitioning strategy, accommodating gradual transitions and overlapping class structure. Using rigorous numerical experiments, our proposed method is demonstrated to outperform state-of-the-art fuzzy clustering approaches for MTS, including fuzzy C-means and variable-based principal component analysis-based clustering. Lastly, we demonstrate the effectiveness of our approach to EEG data where latent cognitive states such as alertness and drowsiness exhibit frequency-specific dynamics and ambiguity. Our method captures both spectral and spatial features by locating the frequency-dependent structure and brain functional connectivity. Built on the KenCoh framework for fuzzy clustering, it handles the complexity of high-dimensional time series data and is broadly applicable to domains such as neuroscience, wearable sensing, environmental monitoring, and finance.

KEY WORDS: neuroscience; robust optimization; spectral dependence; spectral feature; time series data mining

¹King Abdullah University of Science and Technology (KAUST), Computer, Electrical and Mathematical Sciences and Engineering (CEMSE) Division, Thuwal 23955-6900, Saudi Arabia.

*These authors contributed equally to this work.

Correspondence: ziling.ma@kaust.edu.sa, marasherlin.talento@kaust.edu.sa, ying.sun@kaust.edu.sa, her-
nando.ombao@kaust.edu.sa
Preprint. Under review.

1 Introduction

Brain networks, consisting of nodes in brain regions and edges that represent cross-regional interactions or connectivity, are useful to distinguish between control and patient groups, as well as different brain states within an individual (Talento et al., 2024). Clustering brain states based on features extracted from multivariate time series (MTS) of brain signals enables the discovery of distinct neural patterns, identification of cognitive state transitions, and supports personalized, data-driven neuroscience applications (Honey et al., 2007; Van Den Heuvel and Pol, 2010). However, several challenges make this task nontrivial, such as, high dimensionality, temporal dependencies, spectral complexity (Von Luxburg, 2007), and the presence of noise or artifacts (Rodrigues et al., 2017; Ma et al., 2024). These complexity blur the boundaries between brain states and between populations. (Ann Maharaj et al., 2010; Izakian et al., 2015). As a consequence, brain functional networks between brain states within an individual (or between populations, e.g., control and disease) become inseparable.

Aside from the underlying states that switch over time (Samdin et al., 2016; Ting et al., 2017), the multivariate time series is often composed of different oscillatory patterns that reflect different latent conditions in the system. Spectral-domain representations provide a principled way to summarize and analyze such signals. Using spectral analysis, we study the dynamic cross-regional interactions between oscillations which contain meaningful structural and functional information (Van Vugt et al., 2007; Ombao and Pinto, 2024). For instance, electroencephalogram (EEG) oscillations in the 13–30 Hz range (measured in Hertz, or cycles per second) exhibit distinct patterns in patients with Parkinson’s disease (Little and Brown, 2014) and driver’s task-based attention (Li et al., 2022). These findings support the idea that specific frequency bands can offer greater discriminatory power for identifying certain brain states. However, EEG signals, are non-invasive brain imaging modality that are susceptible to artifacts such as eye blinks and external distractions (Jiang et al., 2019). Hence, extracting

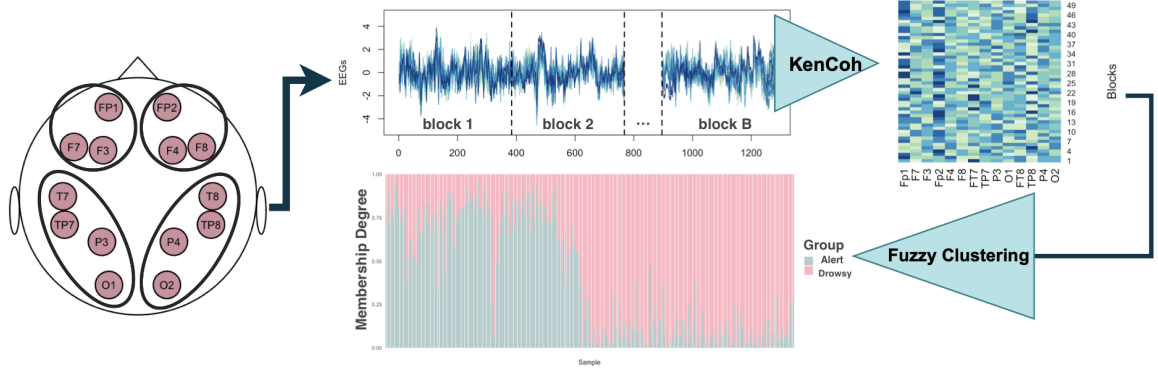


Figure 1: Schematic diagram of the FuzzCoh method. Electroencephalogram (EEG) signals collected from multiple nodes (left panel) are processed through the FuzzCoh pipeline to extract meaningful connectivity patterns.

and categorizing these patterns requires methods that are both robust to noise and flexible in representing overlapping or transitional states.

To address these needs, we propose a robust fuzzy clustering framework in the spectral domain that takes advantage of the robustness of the Kendal’s tau-based canonical coherence (KenCoh) proposed in Talento et al. (2024). KenCoh defined spectral dependence through monotonic canonical relationships between two groups of signals within a specific frequency-band. KenCoh’s ability to quantify spectral dependence across groups of signals enhances the interpretability of multivariate temporal connectivity, e.g., in brain regions where multiple concurrently recorded neural signals reflect localized brain functions. In other words, this technique enables the extraction of coherence-based features that are both interpretable and resistant to distortion by artifacts or outliers.

In our proposed method, spectral features extracted from KenCoh are integrated into a fuzzy clustering framework—hence the name FuzzCoh. Our method permits partial membership assignments that are frequency-based, thereby effectively capturing transitional or mixed-state phenomena frequently observed in real-world datasets. In this article, we demonstrate the effectiveness of the proposed FuzzCoh method using the multi-node, multi-trial EEG data designed to detect whether an individual is in a drowsy or alert state (Cao

et al., 2019). Detecting drowsiness is an especially relevant application, as it has significant safety implications, that is, drowsy driving is implicated in a large fraction of road accidents and fatalities worldwide (Tefft, 2010; Higgins et al., 2017; Filtiness et al., 2017). Drowsiness and alertness are not binary brain states. In fact, there is “fuzziness” between drowsiness and alertness. Drivers frequently experience intermediate or transitional phases of cognitive fatigue (Albadawi et al., 2022). This ambiguity of states makes fuzzy clustering a well-suited approach for modeling the underlying dynamics.

Figure 1 shows the placement of 14 EEG channels on the scalp, including regions near the prefrontal lobe (FP1, FP2), frontal lobe (F3, F4, F7, F8), temporo-parietal lobe (TP7, TP8, T7, T8, P3, P4), and occipital lobe (O1, O2). These regions are associated with brain functionalities that are relevant to driving-task Li et al. (2022). EEG is widely used for monitoring cognitive states, and its spectral properties, particularly in the Delta $\Omega = (0, 4]$ Hz, Theta $\Omega = (4, 8]$ Hz, Alpha $\Omega = (8, 12]$ Hz, Beta $\Omega = (12, 30]$ Hz, and Gamma $\Omega = (30, 50]$ Hz bands, which are closely linked to mental alertness and drowsiness (Klimesch, 1999; Correa et al., 2014; Chaabene et al., 2021). Here, these frequency bands (e.g., Delta-band) are extracted from the signal or time series through filtering (i.e., Butterworth filter) (Ombao and Pinto, 2024). Let $\{X(t)\}_{t=1}^T$ be a weakly-stationary time-series, and let $g(h)$, for $h \in \mathbb{Z}$, be an absolutely summable linear filter, such that, $\sum_{h=-\infty}^{\infty} |g(h)| < \infty$. Then, the filtered series is denoted as $X_{\Omega}(t) := \sum_{h=-\infty}^{\infty} g(t-h)X(t)$. This filtered series $X_{\Omega}(t)$ has zero spectral power outside Ω -band (see Ombao and Pinto, 2024, for details).

While EEG serves as our main case study, the proposed framework is broadly applicable to any domain where frequency-specific dependencies and ambiguous class boundaries are present. Examples include wearable sensor streams, financial volatility cycles, or environmental time series.

The main contributions of this work are as follows:

- (1) We develop a novel fuzzy clustering method in the frequency domain, called FuzzCoh, which identifies frequency bands (or underlying oscillations) that most effectively discriminate between MTS states based on their dependence structure.
- (2) We adopt a robust estimation of multivariate spectral-dependence structure, enabling our method to remain stable and accurately represent the underlying structure of the data, even under severe contamination.
- (3) We demonstrate the advantages of our method on EEG data, where transitional brain states are present and rigid group assignments from hard clustering can be misleading. Additionally, our method provides a pathway for relating brain states to the underlying brain functional-connectivity structure.
- (4) Our method incorporates spatial information, recognizing that the brain consists of distinct regions. By examining the connectivity between regions, we can identify which brain areas show the most pronounced differences between alert and drowsy states.

In summary, our novel rank-based fuzzy clustering approach is broadly applicable to real-world MTS problems, where spatial and spectral information is informative and non-ignorable overlaps in the underlying states are present.

2 Methodology

2.1 Lagged dependence matrix of filtered signals

Consider a non-stationary MTS $\mathbf{Z}_{BT \times (p+q)} = (\mathbf{X}_{BT \times p}, \mathbf{Y}_{BT \times q})$. Suppose that this process is ‘locally stationary’ so that for a block $b, (b = 1, \dots, B)$ of length T , the time series are approximately stationary. Let $\mathbf{Z}_{\Omega}^{(b)}(t) \in \mathbb{R}^{p+q}$ denote the \mathbf{Z}_t corresponding to the b -th block filtered to the Ω frequency band. We define $\mathbf{P}^{(b)}(\Omega, \ell)$ as the b -th block lagged dependence among filtered signals on Ω at lag $\ell = 0, \pm 1, \dots, \pm L$, i.e., $P_{jk}^{(b)}(\Omega, \ell) = f(Z_{\Omega,j}(t), Z_{\Omega,k}(t + \ell)) = f(Z_{\Omega,j}(t - \ell), Z_{\Omega,k}(t))$, for $j, k = 1, \dots, p + q$ (see Talento et al., 2024, for details). The

function $f : \mathbb{R}^2 \rightarrow (-1, 1)$ is defined for $t \neq s = 1, \dots, T - \ell$ as

$$\begin{aligned} \tau^{(b)}(\Omega, \ell) &= \mathbb{E}[\text{sign}\{(Z_{\Omega}^{(b)}(t) - Z_{\Omega}^{(b)}(s))(Z_{\Omega}^{(b)}(t - \ell) - Z_{\Omega}^{(b)}(s - \ell))\}], \\ f(Z_{\Omega,j}(t - \ell), Z_{\Omega,k}(t)) &= \sin\left(\frac{\pi}{2}\tau^{(b)}(\Omega, \ell)\right). \end{aligned} \quad (1)$$

We can subset the lagged dependence matrix into four sub-parts as

$$\mathbf{P}^{(b)}(\Omega, \ell) = \begin{pmatrix} \mathbf{P}_{X,X}^{(b)}(\Omega, \ell) & \mathbf{P}_{X,Y}^{(b)}(\Omega, \ell) \\ \mathbf{P}_{Y,X}^{(b)}(\Omega, \ell) & \mathbf{P}_{Y,Y}^{(b)}(\Omega, \ell) \end{pmatrix}. \quad (2)$$

These four submatrices of $\mathbf{P}^{(b)}(\Omega, \ell)$ are the ingredients in identifying fuzzy series. We now define spectral canonical coherence at block b , denoted as $R_1(b, \Omega)$. The overall measure of spectral association between $\mathbf{X}(t)$ and $\mathbf{Y}(t)$ is defined as

$$R_1(b, \Omega) = \max_{\mathbf{u}_{b,\Omega}, \mathbf{v}_{b,\Omega}} \left\{ \mathbf{u}_{b,\Omega}^{\top} \mathbf{P}_{X,Y}^{(b)}(\Omega, \ell) \mathbf{v}_{b,\Omega} \right\}^2, \quad \text{such that,} \quad (3)$$

$$\mathbf{u}_{b,\Omega}^{\top} \mathbf{P}_{X,X}^{(b)}(\Omega, 0) \mathbf{u}_{b,\Omega} = \mathbf{v}_{b,\Omega}^{\top} \mathbf{P}_{Y,Y}^{(b)}(\Omega, 0) \mathbf{v}_{b,\Omega} = 1.$$

These $\mathbf{u}_{b,\Omega}$ and $\mathbf{v}_{b,\Omega}$ are the block-wise canonical variates (see Talento et al., 2024, for details). These vectors show the relative contribution of the variables to the maximum association, $R_1(b, \Omega)$. This paper exploited the structure of connectivity through $\mathbf{u}_{b,\Omega}$ and $\mathbf{v}_{b,\Omega}$ to determine the clusters of multiple time series for a specific oscillation band.

2.2 FuzzCoh: The robust fuzzy clustering algorithm based on KenCoh

2.2.1 The clustering procedures

We use the standardized canonical directions, $\mathbf{u}_{b,\Omega}$ and $\mathbf{v}_{b,\Omega}$, which are computed from the filtered signals $\mathbf{X}_{\Omega}^{(b)} \in \mathbb{R}^{T \times p}$ and $\mathbf{Y}_{\Omega}^{(b)} \in \mathbb{R}^{T \times q}$, and capture the maximum cross-dependence at a given spectral band Ω , as spectral features to conduct the fuzzy clustering.

Consider a filtered MTS dataset consisting of B realizations, denoted by $\mathbf{Z}_{\Omega} = \{\mathbf{Z}_{\Omega}^{(1)}, \dots, \mathbf{Z}_{\Omega}^{(B)}\}$.

Also, let $\mathbf{Z}_\Omega^{(b)}$ be the concatenation of realizations $\mathbf{X}_\Omega^{(b)} \in \mathbb{R}^{T \times p}$ and $\mathbf{Y}_\Omega^{(b)} \in \mathbb{R}^{T \times q}$, that is,

$$\mathbf{Z}_\Omega^{(b)} = \left(\mathbf{X}_\Omega^{(b)}, \mathbf{Y}_\Omega^{(b)} \right),$$

for $b = 1, \dots, B$. Moreover, denote $\mathbf{d}_b^\Omega = (|\mathbf{u}_{b,\Omega}^\top|, |\mathbf{v}_{b,\Omega}^\top|)^\top \in \mathbb{R}^{p+q}$, where $|\cdot|$ is the absolute-value operator, applied element-wise to a vector. It concatenates the element-wise absolute values of the standardized canonical directions obtained at frequency band Ω and b -th series.

We compute this for each MTS object to obtain a collection of $\{\mathbf{d}_b^\Omega\}_{b=1}^B$, denoted as $\mathbf{d}^\Omega = \{\mathbf{d}_1^\Omega, \dots, \mathbf{d}_B^\Omega\}$. Then we perform a fuzzy C -means clustering model using \mathbf{d}^Ω , aiming to find a set of cluster centers $\bar{\mathbf{d}}^\Omega = \{\bar{\mathbf{d}}_1^\Omega, \dots, \bar{\mathbf{d}}_C^\Omega\}$, and the $B \times C$ fuzzy coefficient matrix, $\mathbf{E} = (e_{bc}^\Omega)$, for $b = \{1, \dots, B\}$ and $c = \{1, \dots, C\}$, by solving the minimization problem

$$\begin{cases} \min_{\bar{\mathbf{d}}^\Omega, \mathbf{E}} \sum_{b=1}^B \sum_{c=1}^C (e_{bc}^\Omega)^m \left\| \mathbf{d}_b^\Omega - \bar{\mathbf{d}}_c^\Omega \right\|^2, \\ \text{subject to } \sum_{c=1}^C e_{bc}^\Omega = 1, \quad e_{bc}^\Omega \geq 0, \quad \forall b = 1, \dots, B. \end{cases} \quad (4)$$

Here, $e_{bc}^\Omega \in [0, 1]$ represents the membership degree of the b -th series to the c -th cluster, and $m > 1$ is the fuzziness parameter controlling the degree of fuzziness of the partition.

The optimization problem in Equation 4 is solved via an iterative procedure. The update formula for the membership takes the form

$$e_{bc}^\Omega = \left(\sum_{c'=1}^C \left(\frac{\left\| \mathbf{d}_b^\Omega - \bar{\mathbf{d}}_{(c)}^\Omega \right\|^2}{\left\| \mathbf{d}_b^\Omega - \bar{\mathbf{d}}_{(c')}^\Omega \right\|^2} \right)^{\frac{1}{m-1}} \right)^{-1}, \quad (5)$$

and for the centers, we have

$$\bar{\mathbf{d}}_c^\Omega = \frac{\sum_{b=1}^B (e_{bc}^\Omega)^m \mathbf{d}_b^\Omega}{\sum_{b=1}^B (e_{bc}^\Omega)^m}. \quad (6)$$

2.2.2 The cluster validity index for the automatic selection of C and m

As stated by Rhee and Oh (1996), if fuzzy cluster analysis is to make a significant contribution to engineering applications, greater attention must be given to the fundamental decision of

determining the number of clusters in the data. In this paper, we present a cluster validity index (CVI) to help determine the optimal selection of C . We adopt the Fuzzy Silhouette index (FSI) (Rawashdeh and Ralescu, 2012), which generalizes the classical silhouette index (Rousseeuw, 1987) to the fuzzy setting. For each MTS object d_b^Ω , the silhouette value with respect to cluster c is computed as

$$s_{bc}^\Omega = \frac{n_{bc}^\Omega - a_{bc}^\Omega}{\max(a_{bc}^\Omega, n_{bc}^\Omega)}, \quad (7)$$

where a_{bc} is the average dissimilarity between d_b^Ω and all other objects in cluster c , weighted by their membership degrees, defined as,

$$a_{bc}^\Omega = \frac{\sum_{j \neq b} (e_{jc}^\Omega)^m \cdot \|d_b^\Omega - d_j^\Omega\|}{\sum_{j \neq b} (e_{jc}^\Omega)^m}, \quad (8)$$

and n_{bc} is the minimum average dissimilarity between d_b^Ω and all objects in another cluster $c' \neq c$, defined as,

$$n_{bc}^\Omega = \min_{c' \neq c} \left(\frac{\sum_{b=1}^B (e_{bc'}^\Omega)^m \cdot \|d_b^\Omega - d_j^\Omega\|}{\sum_{b=1}^B (e_{bc'}^\Omega)^m} \right). \quad (9)$$

The overall FSI, for a specific frequency band Ω , is then given by,

$$\text{FSI}_\Omega = \frac{1}{B} \sum_{b=1}^B \sum_{c=1}^C (e_{bc}^\Omega)^m \cdot s_{bc}^\Omega. \quad (10)$$

A higher FSI_Ω value indicates that the fuzzy memberships align well with the underlying cluster structure, reflecting compact and well-separated clusters with minimal ambiguity in membership assignments. Therefore, when no prior knowledge is available for a given dataset, we recommend performing a grid search. For example, $C \in \{2, 3, \dots, 6\}$, as suggested in Ferraro et al. (2019), and $m \in [1.2, 2.5]$ (a common range for the fuzziness parameter), and selecting the configuration that yields the highest FSI. However, as in our simulation and

real data application, we focus on detecting two different brain states, i.e., drowsy and alert. Thus, we fix $C = 2$ in our paper.

3 Simulation

In this section, we assess the performance of FuzzCoh by generating heavy-tailed fuzzy multivariate time series based on the simulated examples in Talento et al. (2024). We begin with a mixture of second-order autoregressive processes (AR(2)) for different blocks, that is, for eight channels/time series ($p = 4$ and $q = 4$) we have

$$\begin{pmatrix} \mathbf{X}^{(b)}(t) \\ \mathbf{Y}^{(b)}(t) \end{pmatrix} = [\mathbf{A}_1 D^{(b)}(t) + \mathbf{A}_0 (1 - D^{(b)}(t))] \mathbf{O}^{(b)}(t) + \mathbf{W}^{(b)}(t) \quad (11)$$

where $\mathbf{X}^{(b)}(t) \in \mathbb{R}^p$ and $\mathbf{Y}^{(b)}(t) \in \mathbb{R}^q$ are the concatenated multivariate time series at block b . The vector of latent processes, $\mathbf{O}^{(b)}(t) \in \mathbb{R}^5$, is composed of different mutually exclusive AR(2)'s. The parameters of $O_r^{(b)}(t)$, for $r = 1, \dots, 5$, are $\phi_{1,r} = 2 \exp(-M) \cos(2\pi\omega_r)$ and $\phi_2 = -\exp(-2M)$, where $M = 1.05$, $S\omega_r \in \{2, 6, 10, 20, 40\}$ and $S = 128$ Hz (settings are followed from Talento et al., 2024). Observe that $S\omega_r$ belongs to any of the five frequency bands defined in Section 2 (details can be found in Ombao and Pinto, 2024).

The fuzzy series are generated through binary indicator, $D^{(b)}(t) = c$, for $c \in \{0, 1\}$. That is, we generate MTS with mixing-matrix $\mathbf{A}_c \in \mathbb{R}^{(p+q) \times 5}$ if time point, t , belongs to cluster- c . This formulation allows us to create blocks of multivariate time series that exclusively belong to one of the two clusters, as well as blocks that contain contributions from both processes, i.e., representing fuzzy series. The b -th multivariate time series is said to be pure if $D^{(b)}(1) = D^{(b)}(2) = \dots = D^{(b)}(T) = c$ and $c \in \{0, 1\}$. The b -th multivariate time series is said to be fuzzy if $\mathbb{P}[D^{(b)}(t) = 0] \in (0, 1)$ and $\mathbb{P}[D^{(b)}(t) = 1] = 1 - \mathbb{P}[D^{(b)}(t) = 0]$ for all $t = 1, \dots, T$.

We provide here four examples that are different in terms of the independent white-noise processes, $\mathbf{W}(t) \in \mathbb{R}^{p+q}$. We let the marginal distribution of white noise processes to have the

following distributions, namely, (i) Example 1: $W_p^{(b)}(t) \sim N(0, 1)$; (ii) Example 2: $W_p^{(b)}(t) \sim$ Student's t_3 ; and (iii) Example 3: $W_p^{(b)}(t) \sim$ Student's t_1 . Examples in (ii) and (iii) are known to be heavy-tailed and example in (iii) has non-existence of second moment. In this paper, a single block consists of 384 time points, i.e., 128 Hz sampling rate for 3 seconds. Moreover, we have $B = 300$ yielding $115,200 \times 8$ data points. The runtime for the whole framework in Figure 1 with this amount of data takes about 2 minutes. The codes are available in the Supplementary Material and implemented in parallel-run.

3.1 Comparison of methods and evaluation indicators

To show the performance of our proposed method, we include two additional methods for comparison.

- (1) Fuzzy C -means (FCM) clustering. FCM is the extension of K -means by allowing each observation to belong to every cluster with a graded membership (Bezdek et al., 1984). The method can be found in the R package [dtwclust], with the function [tsclust].
- (2) Variable-based Principal Component Analysis (VPCA) clustering. It reduces MTS data by applying PCA across the variable dimension, yielding a compact set of variable-wise components that preserve spatial correlations for efficient downstream clustering. The method can be found in the R package [mlmts], with the function [vpca.clustering] (He and Tan, 2018).

As we work with fuzzy partitions, a membership threshold is required to assign each MTS to a specific cluster (López-Oriona et al., 2022; Ma et al., 2025). Because the experiment distinguishes only between the drowsy and alert states, we fix the number of clusters at $C = 2$. Following a standard convention, the b -th series (block) is assigned to cluster c whenever its membership exceeds the cut-off, $e_{bc}^\Omega > 0.7$. For the generated switching series, designed to retain certain membership in both clusters, we deem the allocation correct when $\max\{e_{b1}^\Omega, e_{b2}^\Omega\} < 0.7$, thereby recognizing their intrinsically fuzzy status (Maharaj and D'Urso, 2011; D'Urso and Maharaj, 2012).

After assigning each block a clear label, we use the Rand index (RI) to compare the results of different methods. The RI measures the concordance between our clustering partitions and the true labels:

$$RI = \frac{TP + TN}{TP + TN + FP + FN}, \quad (12)$$

where TP and TN are the numbers of correctly clustered and correctly separated pairs, respectively, while FP and FN represent misclustered pairs. RI has range $[0, 1]$. Higher RI values indicate greater similarity between the experimental and true partitions. This setup allows us to evaluate our proposed clustering method under both well-separated and partially overlapping time-series dynamics.

The results are shown in Figure 2, where we present the mean Rand Index (RI) of the three methods across 100 replications on the same dataset, using different fuzziness parameters. Since the FCM and VPCA methods cannot produce fuzzy clustering by band, we apply all three methods (FCM, FuzzCoh and VPCA) to the raw MTS without feature extraction from specific frequency bands.

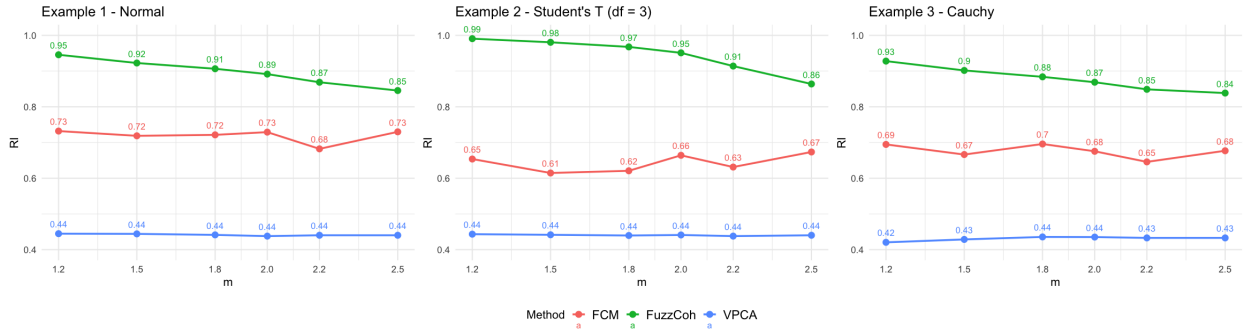


Figure 2: The RI comparison

Figure 2 shows that FuzzCoh consistently maintained high accuracy, even in the presence of heavy-tailed noise, outperforming the other two methods. In contrast, FCM exhibited declining accuracy as noise distribution becomes more heavy, while VPCA performed the worst in terms of Rand Index (RI). Moreover, VPCA fails to converge in at least 50% of cases

when the added noise follows a Cauchy distribution. These results highlight the robustness of FuzzCoh to extreme values and its effectiveness as a leading fuzzy clustering algorithm for multivariate time series.

4 Application

In this section, we evaluate the performance of our method using a real EEG dataset, which is publicly available at https://figshare.com/articles/dataset/EEG_driver_drowsiness_dataset/14273687?file=30707285. The dataset contains 2,022 trials of EEG recording collected from 11 individuals during a simulated driving task. Each trial consists of 384 time points (corresponding to 3 seconds at a sampling rate of 128 Hz), with each trial labeled as either drowsy or alert, i.e., $C = 2$. We emphasize that our method accommodates more than two brain states; however, for the purposes of this application, we fix $C = 2$. In our application, we defined four regions that are shown to be related with driving-task (Li et al., 2022; Talento et al., 2024), namely, (i) left frontal and pre-frontal lobe (LFp), (ii) right frontal and pre-frontal lobe (RFp), (iii) left temporo-parietal and occipital lobe (LTPO) and (iv) right temporo-parietal and occipital lobe (RTPO) (see leftmost panel of Figure 1). Our goal here is to address the following research questions:

- (1) What essential insights on brain networks can we uncover, beyond those offered by hard clustering methods, without compromising clustering accuracy?
- (2) Which frequency band best distinguishes between alert and drowsy states?
- (3) Which pair of brain regions exhibits the most distinct connectivity between the two brain states?

The last two questions reveal a key limitation of temporal-domain clustering methods. In contrast, our spectral approach identifies discriminative frequency bands and quantifies brain region connectivity, offering deeper insights into spatial interactions.

Table 1 presents the maximum RI per subject obtained under two settings: (i) using all

connectivity vectors (i.e., all four brain regions predefined in Figure 1), within a specified frequency band, and (ii) selecting a pair of brain region within a specific frequency band that yields the highest accuracy per subject. The number of trials for each subject is also reported. The accuracy is evaluated against the labels defined by the experimenters based on the driver’s reaction time (see Cao et al., 2019, for details), which we treat as the ground truth. To have a label that can compare with the true label (i.e., ground truth), we assign the time series to the group using the maximum membership rule. For each configuration, we report the corresponding frequency band, accuracy, and the fuzziness parameter m that yield the best results, together with the number of fuzziness time series we detected using a 0.7 threshold.

4.1 All Subject Analysis

From the frequency-band-based analysis, we observe that the Beta and Gamma bands frequently achieve the highest clustering accuracy across subjects. Notably, Beta is the most dominant, yielding the best performance for 5 out of 11 subjects. This observation is consistent with neurophysiological findings: Beta activity (12–30 Hz) is associated with active thinking, alertness, and focused cognitive processing—states that are typically diminished during drowsiness (Sugumar and Vanathi, 2017). Similarly, Gamma activity (above 30 Hz) reflects higher-order mental functions, such as attention and sensory integration, which also deteriorate as the brain transitions into drowsy or unconscious states (Newson and Thiagarajan, 2019). Therefore, these bands naturally capture discriminative features that separate alert and drowsy states, explaining their superior performance in our clustering framework.

The results that incorporate brain region connectivity provide additional interpretability by linking clustering metrics to underlying neural functions. Subject 6 and Subject 7 achieve their best accuracy using Theta band signals from the LFp–RTPO and LFp–RFp

connections, respectively. This pattern highlights the pivotal role of the LFp in distinguishing between alert and drowsy states. The LFp is known to support working memory, executive functions, and language processing—core cognitive domains that are sensitive to fluctuations in mental alertness (Beauchamp, 2005). It plays a central role in goal-directed behavior, planning, and error monitoring, and is structurally connected to other regions such as the temporal and occipital cortices. These connections, particularly with RTPO (associated with sensory integration) and RFp (involved in cognitive control), may reflect the breakdown of coordinated top-down regulation as alertness declines. Thus, the prominence of LFp connectivity in achieving high clustering accuracy suggests that changes in executive and attentional networks are key markers of cognitive state transitions.

Table 1: Max RI per subject by frequency band and regional connectivity, with trial counts

Subj	Number of Trials	RI (%)	Band	m	Fuzzy series (%)	Connectivity	RI (%)	Band	m	Fuzzy series (%)
Subj6	166	94.57	Theta	1.2	15.06	LFp-RTPO	85.54	Theta	2.2	8.43
Subj2	132	88.64	Theta	1.2	5.30	LFp-LTPO	89.39	Beta	1.2	0.00
Subj9	314	87.57	Beta	1.8	62.42	LFp-RFp	81.84	Beta	2.2	16.24
Subj5	224	86.61	Beta	1.2	13.39	LFp-LTPO	79.46	Beta	1.2	1.79
Subj11	226	80.97	Beta	1.8	9.73	RFp-RTPO	74.33	Theta	1.8	1.77
Subj10	108	75.92	Gamma	1.5	13.89	LFp-RFp	76.85	Gamma	2.2	4.62
Subj1	188	75.53	Alpha	1.5	33.51	LFp-RFp	78.72	Beta	1.2	5.31
Subj4	148	67.57	Beta	2.5	17.57	LFp-RFp	67.57	Gamma	1.8	18.24
Subj3	150	67.33	Beta	1.2	14.00	RFp-RTPO	70.67	Gamma	1.2	6.00
Subj8	264	66.29	Gamma	1.2	16.67	LFp-LTPO	62.87	Alpha	2.0	11.36
Subj7	102	65.69	Gamma	1.2	21.57	LFp-RFp	73.53	Theta	2.2	3.92

4.2 Individual Subject Analysis

We further investigate the signals for Subject 2 and Subject 6, which show relatively high RI, i.e., high separation of two states (see Table 1). Subject 2 has $m = 1.2$ fuzziness parameter which indicates that the MTS are well-separable, while Subject 6 has $m = 2.2$ fuzziness parameter for LFp-RTPO suggesting presence of fuzzy MTS.

Subject 2. Figure 3 presents the clustering performance of Subject 2 across different brain region pairs and frequency bands, evaluated under varying fuzziness values m . The subplot labeled “All Regions” shows a clear degradation in clustering quality as m increases,

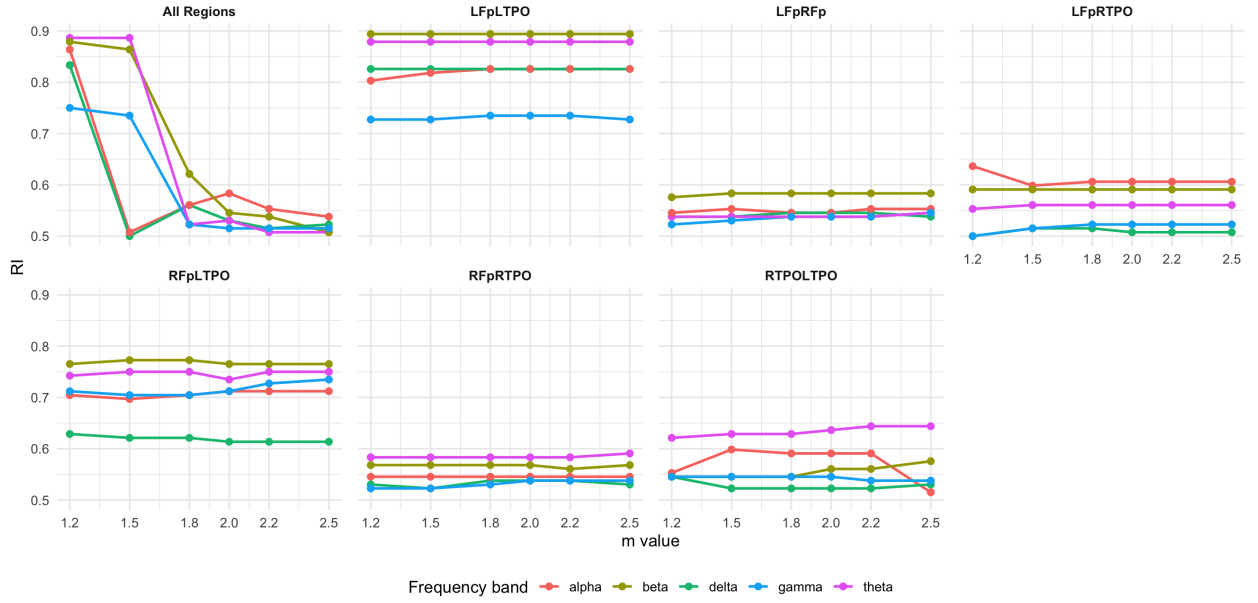


Figure 3: The RI of all or partial brain regions, frequency band, and m value of subject 2

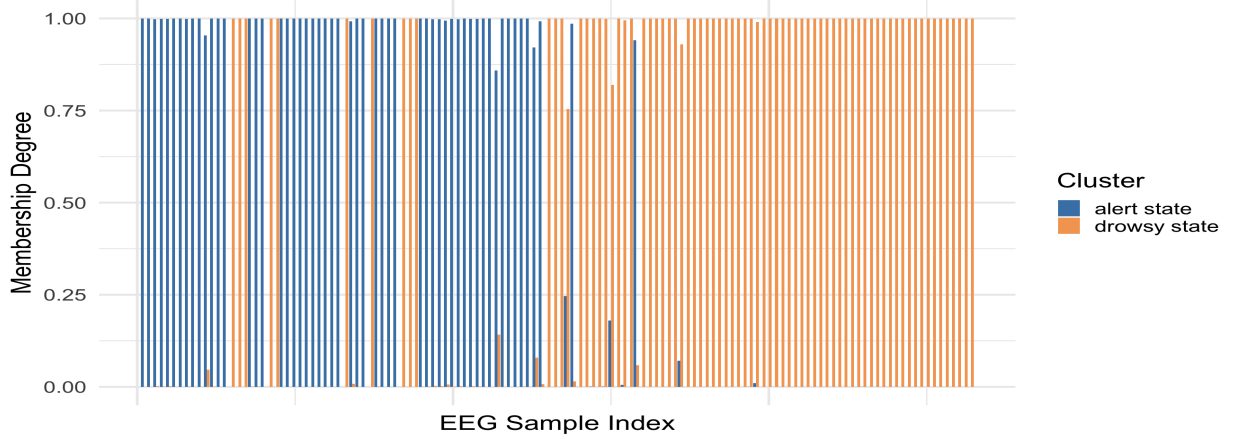


Figure 4: Membership matrix of EEG samples collected from Subject 2 at Beta-band using LFp-LTPO connectivity

indicating sensitivity to the fuzziness parameter when all connections are used. In contrast, specific region pairs such as LFp-LTPO maintain high and stable RI values across all m values, particularly in the Beta and Theta bands. This robustness highlights that selecting meaningful regional connectivity can significantly enhance clustering consistency. Notably, LFp-LTPO outperforms all other pairs, suggesting it captures strong, stable coherence patterns that distinguish between cognitive states for Subject 2. This underlines the importance of targeted connectivity analysis in improving spectral clustering outcomes. Figure 4 plots

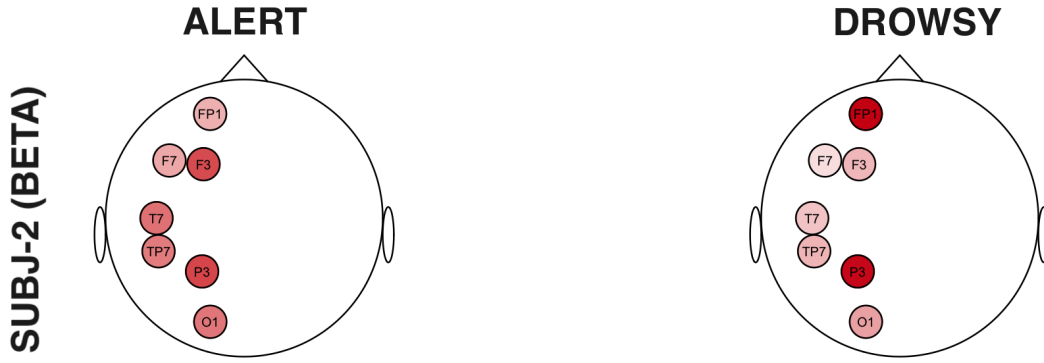


Figure 5: Discriminating functional brain connectivity structure (LFp-LTPO) of Subject 2 at Beta band when **alert** and when **drowsy**

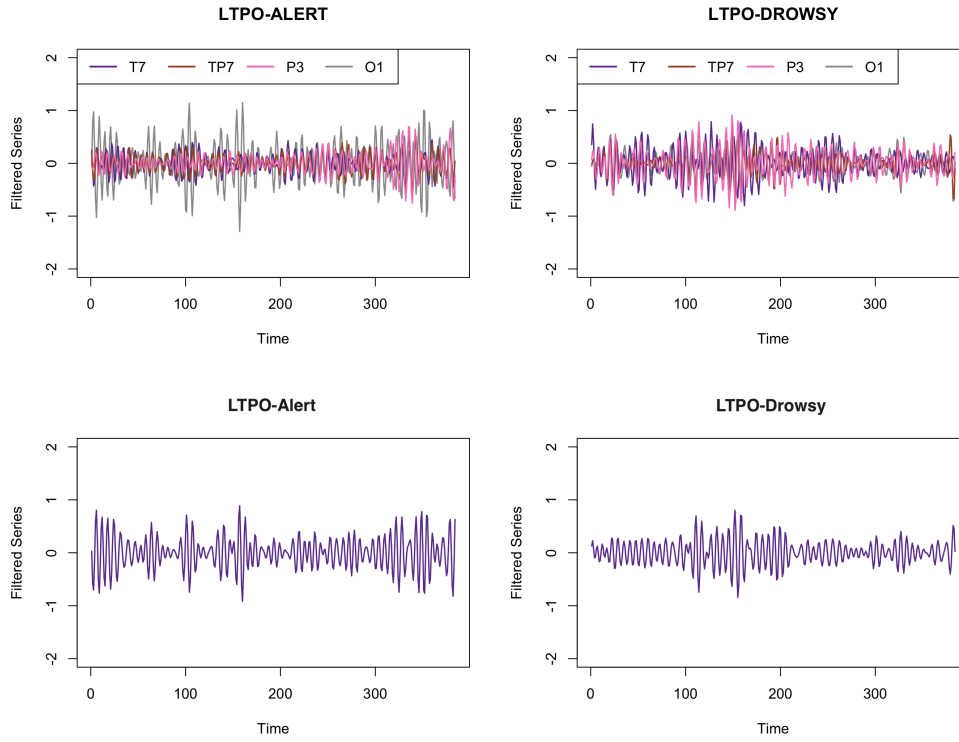


Figure 6: (Top) Filtered signals and (bottom) **summary** of filtered signals from LTPO region during alert and drowsy states at Beta band of Subject 2

the membership matrix for each subject 2 EEG trial by specifying $m = 1.2$ in the Beta band using LFp-LTPO connectivity. Each vertical bar represents the membership of a trail to two clusters: alert state (blue) and drowsy state (orange). The high bars indicate a strong

association with the corresponding state. We can notice that all EEG trails have a high membership in a certain brain state, indicating that the percentage of fuzzy series is 0 %.

Figure 5 shows the LFP–LTPO functional connectivity of Subject 2 in the Beta band for the two brain states. Since Table 1 suggests that Subject 2 has no fuzzy series when using regional connectivity, we only show the figure with the discriminating functional brain connectivity. In the alert state (left panel), the connectivity pattern is dominated by frontal and parietal channels F3 and P3, whereas in the drowsy state (right panel), the hub shifts toward the midline and fronto-polar region, with FP1 and P3 becoming the most central nodes.

Figure 6 shows how the discriminating brain connectivity in the LTPO region changes between the alert and drowsy states for Subject 2. The top row (multichannel view) shows traces for channels T7, TP7, P3 and O1 are overlaid for the alert (left) and drowsy (right) segments. In the alert epoch, pronounced amplitude bursts appear around times 0 and 200, especially on FP1 and F3. These bursts are markedly weaker in the drowsy epoch, signalling reduced Beta power and synchrony. The bottom row (single-lead summaries) summarizes the filtered signals in each state. The alert trace exhibits higher-amplitude Beta oscillations, whereas the drowsy trace shows a lower-energy, more homogeneous rhythm. Moreover, more channels are contributing to the overall association at the Beta band during the alert state than during the drowsy state. Kamiński et al. (2012) found that increased alertness is accompanied by higher EEG activation in the Beta band.

Subject 6. We show the RI across different brain region pairs, frequency bands, and fuzziness values m for Subject 6 in detail, as shown in Figure 7. Beta, Theta, and Gamma bands consistently yield higher RI, indicating strong discriminative power for distinguishing alert and drowsy states. Figure 8 presents the membership matrix using Theta-band signals and all brain regions with $m = 2.2$. Unlike in Figure 4, now some EEG trials exhibit

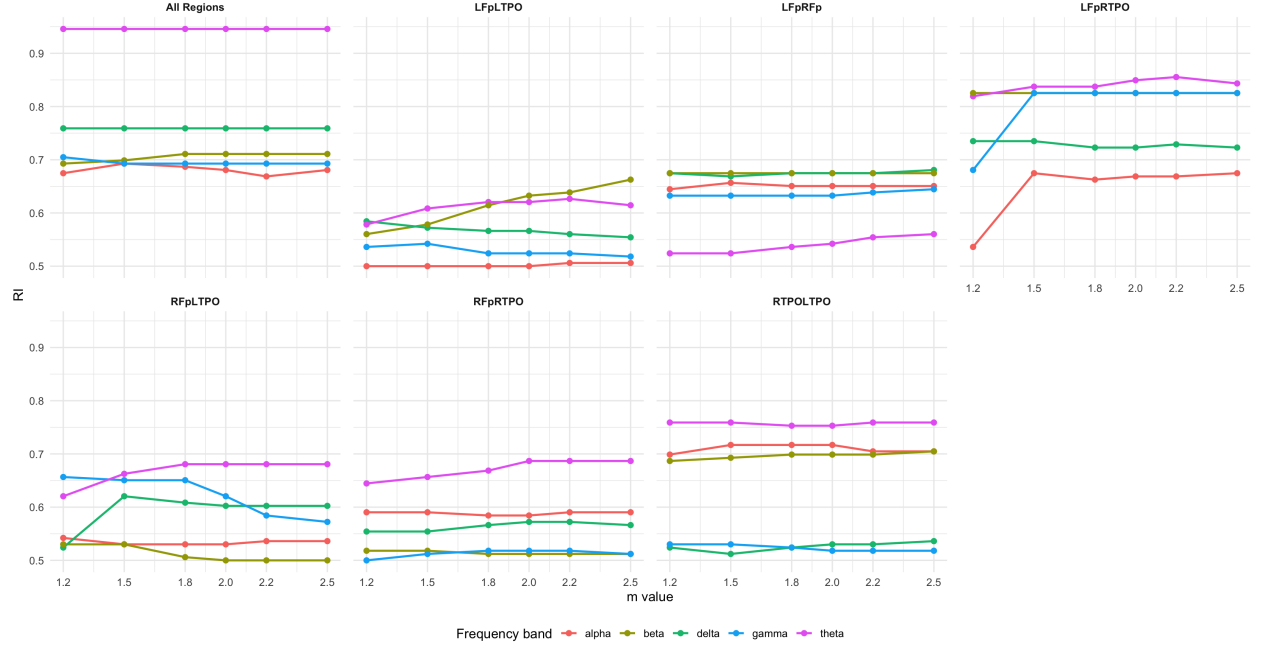


Figure 7: The RI of all or partial brain regions, frequency band, and m value of Subject 6

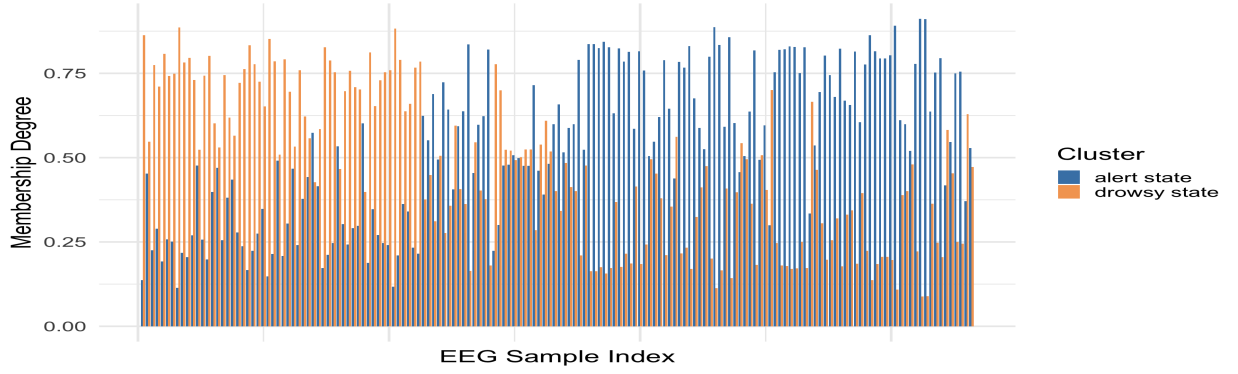


Figure 8: Membership matrix of EEG samples collected from Subject 6 at Theta-band using LFp–RTPO connectivity

substantial membership in both clusters, indicating the presence of a transitional cognitive state between alertness and drowsiness. This underscores the need to detect and analyze such intermediate stages, which are often missed by hard clustering approaches. This flexibility improves clustering quality by accommodating uncertainty and enabling the detection of subtle shifts in cognitive states.

As suggested in Table 1, analyzing the regional connectivity, FuzzCoh suggests 8.43% of its EEG trails are fuzzy series. We would like to visualize both the discriminating and

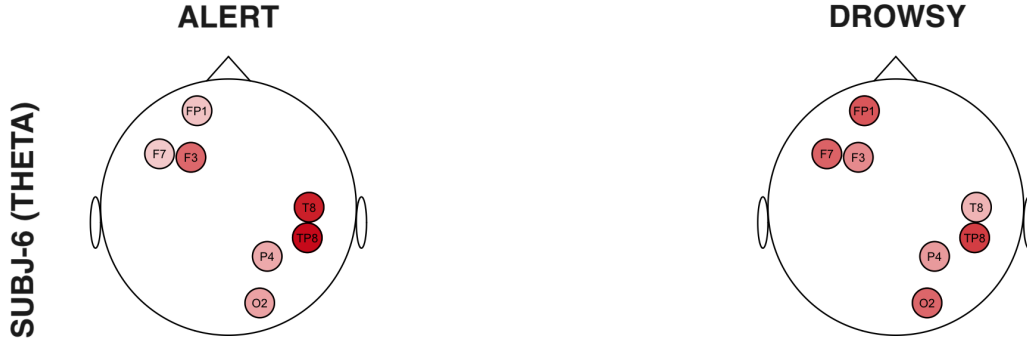


Figure 9: Discriminating functional brain connectivity structure (LFP-RTPO) of Subject 6 at Theta band when **alert** and when **drowsy**

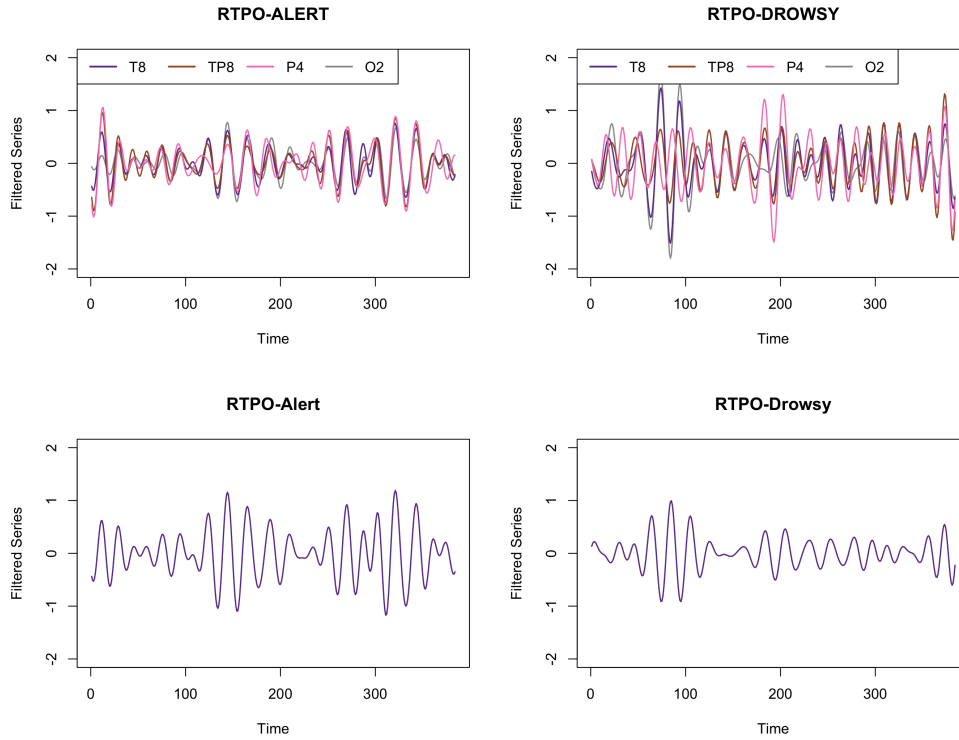


Figure 10: (Top) Discriminating filtered signals from RTPO region during alert and drowsy states and (bottom) their corresponding **summaries** of Subject 6

fuzzy scenarios. Figures 9 and 10 present the non-fuzzy observations and clearly highlight the distinctions between the two brain states. These observations accord with earlier work: Brown et al. (2012) reported a shift toward strong anterior Theta rhythms at the onset of drowsiness, and Sturm et al. (1999) identified evidence for a fronto-parietal-thalamic-brainstem network in the right hemisphere during alertness of 15 individuals



Figure 11: Fuzzy functional brain connectivity structure of Subject 6 at Theta band when **alert** and when **drowsy**

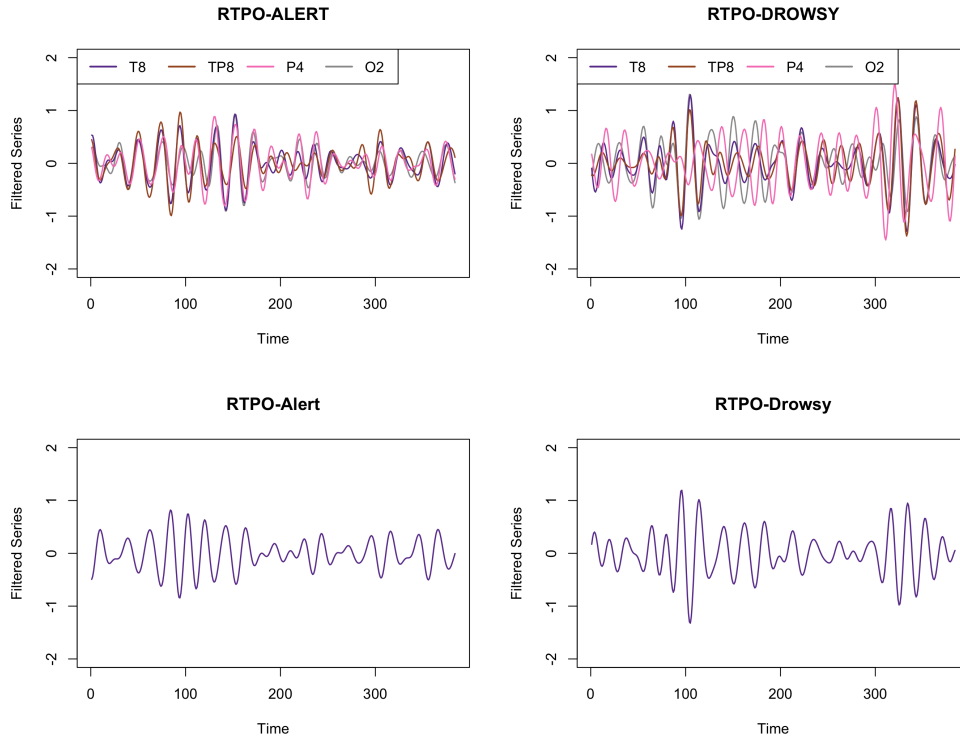


Figure 12: (Top) Fuzzy filtered signals from RTPO region during alert and drowsy states and (bottom) their corresponding **summaries** of Subject 6

The most informative insight comes from the fuzzy cases. Figure 11 shows the fuzzy functional connectivity of Subject 6 in the Theta band. Unlike the discriminating trials, the two states display nearly identical connectivity: every node appears in both maps with comparable intensity, and no channel clearly dominates. Figure 12 plot the corresponding filtered

time series for RTPO region. The waveforms and amplitudes are virtually indistinguishable between the alert (left) and drowsy (right) windows, underscoring the ambiguous nature of these trials. Their connectivity does not align decisively with either cluster, suggesting they represent a transitional or mixed brain state rather than a distinct condition.

Overall, these results suggest that both frequency-specific and connectivity-specific information contribute meaningfully to distinguishing between drowsy and alert brain states. Moreover, tuning the fuzziness parameter m plays an important role in optimizing clustering performance by balancing cluster separation and membership uncertainty. Importantly, by employing a fuzzy clustering framework, we are also able to capture transitional or mixed cognitive states, where the brain activity may not be fully classified as either drowsy or alert. This capacity to represent ambiguity in cluster membership is particularly valuable for modeling the gradual and continuous nature of cognitive state changes observed in EEG data.

5 Discussion

This paper introduced a robust spectral feature-based fuzzy clustering algorithm for multivariate time series, with a specific focus on EEG data. We began by introducing the concept of canonical variates and then formulated the clustering problem in detail. Through comparisons with two alternative methods across various (un)contamination scenarios, we demonstrated that our approach consistently outperforms the others in all cases. The main advantages of our FuzzCoh are: (1) resistant to EEG artifacts, (2) assigns graded memberships to capture the alert-to-drowsy transition, (3) operates in the frequency domain while explicitly modeling functional brain connectivity, and (4) by focusing on specific brain regions, our method performs dimension reduction, enabling clustering on high-dimensional time series data using only relevant channels. In short, by concentrating on a few discriminative frequency bands (Theta, Beta, and Gamma) and key fronto-parietal connections,

our approach markedly sharpens the contrast between brain states, enabling earlier and more reliable drowsiness detection that strengthens driver-monitoring systems, enhances road safety, and benefits other spectral-spatial MTS applications.

Beyond its methodological strengths, our approach offers practical value across domains. In driver drowsiness detection, it enables early-warning systems by capturing subtle shifts in spectral and spatial EEG patterns (Stancin et al., 2021). In clinical diagnostics, it may help differentiate neurological disorders through changes in brain connectivity (Smith, 2005). For neuromarketing and cognitive workload assessment, it extracts interpretable features that reflect mental effort and engagement levels (Dehais et al., 2020).

Except for neuroscience, the FuzzCoh framework can be applied to financial time series by clustering coherence among asset groups to identify market regimes and systemic risk (Haldane and May, 2011; Biase and D’Apolito, 2012), or detect anomalies in cryptocurrency markets (Pocher et al., 2023) by capturing coordinated behavior across tokens at multiple frequencies. In environmental monitoring, it supports clustering of sensor networks (e.g., air quality or temperature) based on shared temporal patterns, enabling early detection of abnormal or synchronized environmental changes (Yin and Gaber, 2008).

By modeling both frequency- and region-specific dependencies within a robust fuzzy clustering framework, FuzzCoh serves as a versatile and interpretable tool for analyzing high-dimensional, multivariate systems in real-world contexts.

Despite its advantages, FuzzCoh remains sensitive to parameter tuning. It also assumes local stationarity, an assumption that may not hold in practice. Furthermore, its reliance on predefined regions and frequency bands can limit generalizability. Future work will therefore: (1) develop adaptive block segmentation and scalable approximations for large-scale MTS, (2) extend FuzzCoh to handle non-stationary MTS, and (3) generalize FuzzCoh for robust detection of outliers in MTS.

Acknowledgments

This research was supported by King Abdullah University of Science and Technology (KAUST).

Conflict of interest statement

The authors declare that they have no known competing financial interests or personal relationships that could have appeared to influence the work reported in this paper.

Data availability statement

Data sharing is not applicable to this article, as the datasets used in our paper are already publicly available.

References

- Albadawi, Y., Takturi, M., and Awad, M. (2022). A review of recent developments in driver drowsiness detection systems. Sensors **22**, 2069.
- Ann Maharaj, E., D’Urso, P., and Galagedera, D. U. (2010). Wavelet-based fuzzy clustering of time series. Journal of classification **27**, 231–275.
- Beauchamp, M. S. (2005). See me, hear me, touch me: multisensory integration in lateral occipital-temporal cortex. Current opinion in neurobiology **15**, 145–153.
- Bezdek, J. C., Ehrlich, R., and Full, W. (1984). Fcm: The fuzzy c-means clustering algorithm. Computers & geosciences **10**, 191–203.
- Biase, P. d. and D’Apolito, E. (2012). The determinants of systematic risk in the italian banking system: A cross-sectional time series analysis. International Journal of Economics and Finance **4**, 152–164.
- Brown, R. E., Basheer, R., McKenna, J. T., Strecker, R. E., and McCarley, R. W. (2012). Control of sleep and wakefulness. Physiological reviews .
- Cao, Z., Chuang, C.-H., King, J.-K., and Lin, C.-T. (2019). Multi-channel eeg recordings during a sustained-attention driving task. Scientific data **6**, 19.
- Chaabene, S., Bouaziz, B., Boudaya, A., Hökelmann, A., Ammar, A., and Chaari, L. (2021). Convolutional neural network for drowsiness detection using eeg signals. Sensors **21**, 1734.
- Correa, A. G., Orosco, L., and Laciari, E. (2014). Automatic detection of drowsiness in eeg records based on multimodal analysis. Medical engineering & physics **36**, 244–249.
- Dehais, F., Lafont, A., Roy, R., and Fairclough, S. (2020). A neuroergonomics approach to mental workload, engagement and human performance. Frontiers in neuroscience **14**, 268.
- D’Urso, P. and Maharaj, E. A. (2012). Wavelets-based clustering of multivariate time series.

- Fuzzy Sets and Systems **193**, 33–61.
- Ferraro, M., Giordani, P., and Serafini, A. (2019). fclust: An r package for fuzzy clustering. The R Journal **11**,.
- Filtiness, A. J., Armstrong, K. A., Watson, A., and Smith, S. S. (2017). Sleep-related crash characteristics: Implications for applying a fatigue definition to crash reports. Accident Analysis & Prevention **99**, 440–444.
- Haldane, A. G. and May, R. M. (2011). Systemic risk in banking ecosystems. Nature **469**, 351–355.
- He, H. and Tan, Y. (2018). Unsupervised classification of multivariate time series using vpca and fuzzy clustering with spatial weighted matrix distance. IEEE Transactions on Cybernetics **50**, 1096–1105.
- Higgins, J. S., Michael, J., Austin, R., Åkerstedt, T., Van Dongen, H. P., Watson, N., Czeisler, C., Pack, A. I., and Rosekind, M. R. (2017). Asleep at the wheel—the road to addressing drowsy driving. Sleep **40**, zsx001.
- Honey, C. J., Kötter, R., Breakspear, M., and Sporns, O. (2007). Network structure of cerebral cortex shapes functional connectivity on multiple time scales. Proceedings of the National Academy of Sciences **104**, 10240–10245.
- Izakian, H., Pedrycz, W., and Jamal, I. (2015). Fuzzy clustering of time series data using dynamic time warping distance. Engineering Applications of Artificial Intelligence **39**, 235–244.
- Jiang, X., Bian, G.-B., and Tian, Z. (2019). Removal of artifacts from eeg signals: a review. Sensors **19**, 987.
- Kamiński, J., Brzezicka, A., Gola, M., and Wróbel, A. (2012). Beta band oscillations engagement in human alertness process. International Journal of Psychophysiology **85**, 125–128.

- Klimesch, W. (1999). Eeg alpha and theta oscillations reflect cognitive and memory performance: a review and analysis. Brain research reviews **29**, 169–195.
- Li, X., Yang, L., and Yan, X. (2022). An exploratory study of drivers’ eeg response during emergent collision avoidance. Journal of safety research **82**, 241–250.
- Little, S. and Brown, P. (2014). The functional role of beta oscillations in parkinson’s disease. Parkinsonism & related disorders **20**, S44–S48.
- López-Oriona, Á., D’Urso, P., Vilar, J. A., and Lafuente-Rego, B. (2022). Quantile-based fuzzy c-means clustering of multivariate time series: Robust techniques. International Journal of Approximate Reasoning **150**, 55–82.
- Ma, Z., Lopez Oriona, A., Ombao, H., and Sun, Y. (2024). ROBCPCA: A robust multivariate time series clustering method based on common principal component analysis.
- Ma, Z., López-Oriona, Á., Ombao, H., and Sun, Y. (2025). FCPCA: Fuzzy clustering of high-dimensional time series based on common principal component analysis. arXiv preprint arXiv:2505.07276 .
- Maharaj, E. A. and D’Urso, P. (2011). Fuzzy clustering of time series in the frequency domain. Information Sciences **181**, 1187–1211.
- Newson, J. J. and Thiagarajan, T. C. (2019). Eeg frequency bands in psychiatric disorders: a review of resting state studies. Frontiers in human neuroscience **12**, 521.
- Ombao, H. and Pinto, M. (2024). Spectral dependence. Econometrics and Statistics **32**, 122–159.
- Pocher, N., Zichichi, M., Merizzi, F., Shafiq, M. Z., and Ferretti, S. (2023). Detecting anomalous cryptocurrency transactions: An aml/cft application of machine learning-based forensics. Electronic Markets **33**, 37.
- Rawashdeh, M. and Ralescu, A. (2012). Crisp and fuzzy cluster validity: Generalized intra-inter silhouette index. In 2012 annual meeting of the North American fuzzy information

- processing society (NAFIPS), pages 1–6. IEEE.
- Rhee, H.-S. and Oh, K.-W. (1996). A validity measure for fuzzy clustering and its use in selecting optimal number of clusters. In Proceedings of IEEE 5th International Fuzzy Systems, volume 2, pages 1020–1025. IEEE.
- Rodrigues, J., Belo, D., and Gamboa, H. (2017). Noise detection on ecg based on agglomerative clustering of morphological features. Computers in biology and medicine **87**, 322–334.
- Rousseeuw, P. J. (1987). Silhouettes: a graphical aid to the interpretation and validation of cluster analysis. Journal of computational and applied mathematics **20**, 53–65.
- Samdin, S. B., Ting, C.-M., Ombao, H., and Salleh, S.-H. (2016). A unified estimation framework for state-related changes in effective brain connectivity. IEEE Transactions on Biomedical Engineering **64**, 844–858.
- Smith, S. J. (2005). Eeg in the diagnosis, classification, and management of patients with epilepsy. Journal of Neurology, Neurosurgery & Psychiatry **76**, ii2–ii7.
- Stancin, I., Cifrek, M., and Jovic, A. (2021). A review of eeg signal features and their application in driver drowsiness detection systems. Sensors **21**, 3786.
- Sturm, W., De Simone, A., Krause, B., Specht, K., Hesselmann, V., Radermacher, I., Herzog, H., Tellmann, L., Müller-Gärtner, H.-W., and Willmes, K. (1999). Functional anatomy of intrinsic alertness: evidence for a fronto-parietal-thalamic-brainstem network in the right hemisphere. Neuropsychologia **37**, 797–805.
- Sugumar, D. and Vanathi, P. (2017). Eeg signal separation using improved eemd-fast iva algorithm. Asian Journal of Research in Social Sciences and Humanities **7**, 1230–1243.
- Talento, M. S. D., Roy, S., and Ombao, H. C. (2024). Kencoh: A ranked-based canonical coherence. arXiv preprint arXiv:2412.10521 .
- Tefft, B. C. (2010). Asleep at the wheel: The prevalence and impact of drowsy driving.

- Ting, C.-M., Ombao, H., Samdin, S. B., and Salleh, S.-H. (2017). Estimating dynamic connectivity states in fmri using regime-switching factor models. IEEE transactions on medical imaging **37**, 1011–1023.
- Van Den Heuvel, M. P. and Pol, H. E. H. (2010). Exploring the brain network: a review on resting-state fmri functional connectivity. European neuropsychopharmacology **20**, 519–534.
- Van Vugt, M. K., Sederberg, P. B., and Kahana, M. J. (2007). Comparison of spectral analysis methods for characterizing brain oscillations. Journal of neuroscience methods **162**, 49–63.
- Von Luxburg, U. (2007). A tutorial on spectral clustering. Statistics and computing **17**, 395–416.
- Yin, J. and Gaber, M. M. (2008). Clustering distributed time series in sensor networks. In 2008 Eighth IEEE International Conference on Data Mining, pages 678–687. IEEE.